ATMOSPHERIC ENVIRONMENT: X 13 (2022) 100161

Contents lists available at ScienceDirect

Atmospheric Environment: X

journal homepage: www.journals.elsevier.com/atmospheric-environment-x

Using the inverse dispersion method to determine methane emissions from biogas plants and wastewater treatment plants with complex source configurations

Marcel Bühler [a,b,c,*,1], Christoph Häni [a], Christof Ammann [d], Stefan Brönnimann [b,c], Thomas Kupper [a]

[a] School of Agricultural, Forest and Food Sciences HAFL, Bern University of Applied Sciences, Länggasse 85, 3052 Zollikofen, Switzerland
[b] Oeschger Centre for Climate Change Research, University of Bern, Hochschulstrasse 4, 3012 Bern, Switzerland
[c] Institute of Geography, University of Bern, Hallerstrasse 12, 3012 Bern, Switzerland
[d] Climate and Agriculture Group, Agroscope, Reckenholzstrasse 191, 8046 Zürich, Switzerland

ARTICLE INFO

Keywords:
Anaerobic digestion
Backward Lagrangian stochastic
GasFinder
Open-path tunable diode laser
Source combination

ABSTRACT

Wastewater treatment plants (WWTPs) and biogas plants (BGPs) are significant sources of methane (CH_4), with a combined share of around 40% within the waste sector of the Swiss national emission inventory. We conducted whole-plant CH_4 emission measurements at two WWTPs and four agricultural BGPs in Switzerland using the inverse dispersion method (IDM). This involved open-path concentration measurements up- and downwind of the plant in combination with a backward Lagrangian stochastic (bLS) model. WWTPs in particular consist of multiple CH_4 sources with different areas and emission strengths. For the combination of the individual emission sources in the bLS modelling, three different calculation approaches with different levels of detail were applied: (i) single source over enveloping polygon area, (ii) uniform emission density for all individual source areas, (iii) specified relative weighting of individual sources based on literature data. Average CH_4 emissions for WWTP-1 and WWTP-2 were 0.82 kg h^{-1} and 0.61 kg h^{-1} and scaled to population equivalents (PE) 166 g PE^{-1} y^{-1} and 381 g PE^{-1} y^{-1}, respectively. BGPs CH_4 emissions varied between 0.39 kg h^{-1} and 2.22 kg h^{-1}, corresponding to less than 5% of the plants' CH_4 production. The highest numbers were due to measurements during other than normal operating conditions. The emissions of WWTPs and BGPs comply with literature values. Approach (iii) with source weighting led to a difference of up to 43% for the two WWTPs compared to the assumption of uniform emissions. Furthermore, we demonstrate how multiple open-path concentration measurements can be combined and how the measurements can be corrected for nearby external CH_4 sources not belonging to the investigated plants. The results of the present study contribute to improved emission data from the waste sector.

1. Introduction

Methane (CH_4) is a relevant greenhouse gas (GHG) with a global warming potential 28 times greater than that of carbon dioxide (CO_2). Anthropogenic CH_4 emissions of which agriculture (mainly ruminants and rice paddies), fossil fuel extraction, landfills and waste are the principal sources, account for 50–65% of total CH_4 emissions (Stocker et al., 2013). Within the framework of the revised CO_2 Act and the Kyoto Protocol, Switzerland is obliged to report regularly on the current status of its GHG emissions including CH_4 with regard to the specified reduction targets (FOEN, 2021a). After agriculture, the waste sector is the second most important source of CH_4 emissions in Switzerland. Wastewater treatment plants (WWTPs) and biogas plants (BGPs) are significant sources of CH_4 with a combined share of around 40% within the waste sector (as of 2019) (FOEN, 2021b). WWTPs comprise a mechanical, biological and chemical stage for wastewater treatment (Gujer, 2007), denoted here as water line. Solids removed from the water line during treatment are directed to the sludge line where dewatering, anaerobic digestion and storage of the sludge occur. In WWTPs, CH_4 is mainly produced in the sludge line and in the energy line i.e. combustion

* Corresponding author. School of Agricultural, Forest and Food Sciences HAFL, Bern University of Applied Sciences, Länggasse 85, 3052, Zollikofen, Switzerland.
E-mail address: marcel.buehler@bfh.ch (M. Bühler).
[1] Now at: Department of Biological and Chemical Engineering, Aarhus University, 8200 Aarhus N, Denmark.

https://doi.org/10.1016/j.aeaoa.2022.100161
Received 17 August 2021; Received in revised form 3 February 2022; Accepted 24 February 2022
Available online 28 February 2022

of biogas in the combined heat and power unit (CHP) and biogas storage (Daelman et al., 2012; Delre et al., 2017). In addition to WWTPs, the sewer system is also a significant source of CH_4 within urban water management (Eijo-Río et al., 2015; Mannina et al., 2018). Agricultural biogas plants (BGPs) process manure from livestock production, organic residues from food processing, landscape and garden maintenance, and catering waste. As for WWTPs, the main sources of CH_4 from BGPs are anaerobic digestion, storage of feedstock material and digestates, and the combustion of biogas. The organic waste is fed directly into an anaerobic digester but, in contrast to most WWTPs, there is usually a post-digester and often no balloon for biogas storage.

Measurements of CH_4 emissions from the whole WWTPs based on direct measurements at exhaust pipes or indirectly by means of the tracer gas dispersion method are available. However, the former is based on measuring the flow rates and the concentration of air from exhaust pipes from plants where those parts of a WWTP producing odours are covered, ventilated and their exhaust air undergoes treatment. Nonetheless, not all parts of WWTPs are necessarily covered and thus some WWTP emissions are excluded from the measurements (STOWA, 2010; Daelman et al., 2012). For investigations using the tracer gas dispersion method mobile analysers were used to obtain a cross-section of the downwind plume (Yoshida et al., 2014; Delre et al., 2017; Samuelsson et al., 2018). The analysers were mounted to a car. This implies relatively short measurement periods, i.e. mostly $\leq$5 measurement campaigns over ca. 1 to $\leq$6 h. Thus, whole WWTP emission measurements including all sources over a longer time period are lacking. As for WWTPs, for BGPs, whole plant emission data from extended measurement periods are needed for reliable emission estimates since it can be expected that CH_4 released from BGPs undergoes a distinct variability over time and this might escape measurement campaigns over a few days or even hours.

Measurements with the inverse dispersion method (IDM), which combines concentration measurements up- and downwind of a source with an atmospheric dispersion model, have been successfully conducted to estimate emissions from stationary sources such as whole farms (VanderZaag et al., 2014; Bühler et al., 2021), manure stores (Flesch et al., 2013) and BGPs (Flesch et al., 2011; Reinelt et al., 2017; Hrad et al., 2021). These studies have highlighted the flexibility in the application of IDM measurements of various sources. Thus, the IDM is a promising option to conduct whole plant emission measurements of WWTPs over a period of several weeks.

In the present study, we conducted CH_4 emissions measurements over several consecutive days with the IDM deploying open-path CH_4 measurements and a backward Lagrangian stochastic (bLS) model at two WWTPs and four agricultural BGPs in Switzerland. They all represent source configurations of greater complexity because they consist of multiple spatially distributed sources, and/or the measurements were complicated by the influence of other nearby CH_4 sources that needed to be corrected for. We investigated the effect of the complex source distribution and associated uncertainties on the quantification of the total CH_4 emission of the whole plants (WWTP or BGP). For this purpose, different approaches for combining individual sources were compared. It is hypothesised that with an optimised experimental setup, the effect of the distributed multiple sources within the plant is small and that neighbouring external sources can be separated from the emissions of the investigated plant.

2. Material and methodology

2.1. Experimental sites and periods

Measurements were conducted at two WWTPs and four agricultural BGPs in Switzerland. The selected WWTPs and BGPs are common plant types and can be considered representative of plants occurring in Switzerland. In the following, the selected WWTPs and BGPs and their surroundings are explained in detail.

2.1.1. Wastewater treatment plants

WWTP-1 (Table 1, Fig. 1A) is located in a rather flat topography. The only major increase in elevation is a mound from the road crossing the train line and the motorway, situated about 110 m southwest of WWTP-1. Between WWTP-1 and the mound there were 11 heifers grazing. Trees grow along the river northeast of WWTP-1. 300 m northeast of WWTP-1 is a small settlement with several cattle housings (138 head in total). Inside the WWTP-1 area, there is an open storage for road-sweepings covered by a roof (Table 4). WWTP-2 is located in a valley with approximately south-north direction. In the prevailing wind directions at WWTP-2, there are no major obstacles or elevations outside the WWTP area that could potentially influence the turbulence. West of WWTP-2 along the river are trees and 160 m north of WWTP-2 is a small barn with 29 sheep (Fig. 1B, Table 4).

WWTP-1 consists of a conventional activated sludge treatment with complete nitrification and denitrification with open sludge storage tanks. The population equivalent (PE) of WWTP-1 during the measurements was 43,534. WWTP-2 consists of a sequencing batch reactor (SBR) system with complete nitrification and denitrification with open sludge storage tanks. The population equivalent of WWTP-2 during the campaigns was 14,071. For both WWTPs, the sludge is regularly evacuated and transported to a larger WWTP for further treatment and disposal. For both WWTPs the biogas produced in the digester is used in an onsite CHP and part of the heat is used to heat the digester. Further information on the WWTPs is given in Table 1 and the Supporting information 1, section 1. Measurements were conducted continuously between September 23, 2019 and October 14, 2019 at WWTP-1 and between May 6, 2020 and May 20, 2020 at WWTP-2.

Table 1
Operating data and characteristics of the sludge line and energy line as major source of CH_4 for WWTP-1 and WWTP-2. MC: measuring campaign. The total WWTP area corresponds to the orange outlined polygon in Fig. 1.

		WWTP-1	WWTP-2
Name		Moossee-Urtenenbach	Gürbetal
Geographical coordinates		47.05572° N	46.84409° N
		7.53964° E	7.50276° E
Total WWTP area [m^2]		21,803	7,354
Population equivalents (PE)[a]		43,534	14,071
Connected inhabitants		33,126	14,365
Total digester volume [m^3]		2,200	1,400
Gas production during MC [$m^3\ d^{-1}$]		1,261	672
Sludge storage tanks (uncovered)	Total volume [m^3]	1,960	400
	Used volume during MC [m^3]	632	93
	Surface [m^2]	331	64

[a] The PE of WWTP-2 was calculated based on analyses for the first six months of 2020 and not for an entire year as for WWTP-1 which might explain the number of PE being somewhat smaller than that of connected inhabitants. Another reason could be commuters leaving the catchment area during workdays.

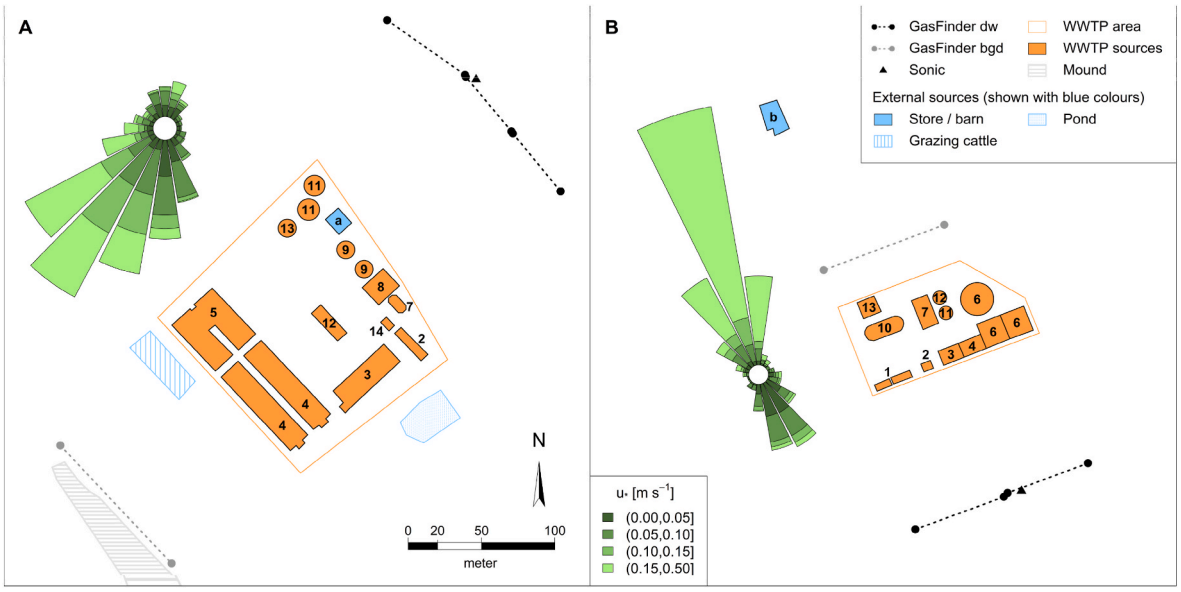

Fig. 1. Schematic overview of the two WWTPs with a wind rose. A = WWTP-1, B = WWTP-2. The wind rose indicates the frequency of occurrence of wind directions and the friction velocity u_* in each wind direction sector. dw = downwind, bgd = background. The name for the numbers indicating the different WWTP sources and the letters indicating external sources from structures are given in Table 4. The height of the mound increases towards southeast.

2.1.2. Biogas plants

Measurements were conducted at four different agricultural BGPs. A schematic overview of each BGP is given in Fig. 2. The agricultural BGPs have at least 80% (by fresh weight) of feedstock input as manure and organic residues of agricultural origin. The remaining amount is organic waste from non-agricultural sources to increase gas production. BGP-1, BGP-3 and BGP-4 have a non-gastight digestate store, while the storage tank of BGP-2 is gastight (Table 2). At all BGPs, there was livestock housing in the close vicinity. At each BGP, the biogas is incinerated in an onsite CHP to produce electricity and heat. The heat is used to heat the digester and other purposes such as heating houses or drying agricultural goods. There was no biogas upgrading or injecting of biogas into gas distribution grids at these four sites.

BGP-1 is located on a slope facing northeast. The average inclination of the slope is about 9%. Southwest of the farm on top of the hill is a small forest. BGP-1 belongs to a farm with dairy cows and heifers. At this site, CH_4 originating from housed and grazing cattle can represent a source of CH_4 that is in a similar order of magnitude as that of the BGP. Next to the farm are residential and farm buildings. During the second campaign (BGP-1.2), the dairy cows and heifers were occasionally grazing on the field northwest of the housing (Fig. 2A). Measurements at BGP-1 were continuously conducted from February 21, 2018 until April 27, 2018 (BGP-1.1) and from May 30, 2019 until June 19, 2019 (BGP-1.2). During the first period, 38 dairy cows and 17 heifers were present and during the second period 28 dairy cows and 16 heifers.

BGP-2 is located in a rather hilly area. However, the elevation differences in a radius of 250 m around the BGP are less than 10 m. Next to BGP-2 is a fattening pig housing and, adjacent to it, a circular slurry tank covered with a tent structure. Northwest of BGP-2, there were non-lactating cows and heifers grazing. In Fig. 2B, only the area within the pasture is denoted, where the animals were resting. Measurements were conducted continuously from June 7, 2018 until July 23, 2018 (BGP-2.1) and July 1, 2019 until July 19, 2019 (BGP-2.2). During both campaigns, there were 380 fattening pigs inside the housing. In the first campaign, 8 non-lactating dairy cows and 8 heifers were grazing and in the second campaign there were 5 non-lactating dairy cows grazing.

BGP-3 is in a valley on a southeast facing slope with an inclination of about 5%. Northwest of BGP-3 is a fattening pig (480 head) farm (livestock housing 2 in Figs. 2C), 300 m southwest is a farm with 59 dairy cows and 33 heifers (livestock housing 1) and 130 m northeast of BGP-3 is a housing with 36 dairy cows, 6 non-lactating dairy cows and 3 heifers (livestock housing 3). Measurements were conducted continuously between December 2, 2019 and December 18, 2019.

BGP-4 is located on a plain. However, directly south of it is a slope with an average inclination of about 7% facing southwest. There is a forest northeast of BGP-4. The farm operating BGP-4 has 91 dairy cows and 46 heifers that were either in the housing or grazing on the pastures around the BGP. Measurements were conducted from August 10, 2018 until September 11, 2018.

2.2. Measurement setup

2.2.1. Methane concentration measurements

CH_4 concentration measurements at all sites were conducted with GasFinder3-OP (Boreal Laser Inc., Edmonton, Canada), which are open-path tunable diode laser spectrometers. As retroreflectors, either seven (BGP-1.1 BGP-2.1, BGP-4) or twelve (WWTP-1, WWTP-2, BGP-1.2, BGP-2.2, BGP-3) corner cubes were used. To reduce data loss due to misalignment of the laser beam with the retroreflectors, the tripods of the GasFinder sensors and retroreflectors were fixed to the ground by a clamping set and a base screw from 2019 onwards (Supporting information 1, section 3). The measured concentration was adjusted for local air temperature and pressure using device-specific relationships determined by factory calibration. The concentrations measured at 0.3–1 Hz were averaged to 30 min periods and periods with data coverage lower than 75% (22.5 min) were excluded.

GasFinder output concentrations have a bias which must be corrected (Häni et al., 2021). Therefore, an offset and span correction of the individual concentration measurements is necessary. This was achieved either with an intercomparison of the utilised GasFinders before or after the campaign by placing the GasFinders in parallel or/and by using wind sectors during the campaigns for which all GasFinders were exposed to the same background concentration (Supporting information 1, section 3). The uncertainty of the utilised GasFinder ranges from 2.1 pmm-m to 10.6 ppm-m (Häni et al., 2021).

2.2.2. Positioning of GasFinders

Harper et al. (2011) recommend placing the GasFinder at least ten times the measuring height of the source. In our case, this corresponds to a concentration fetch of 100–150 m. We generally planned the

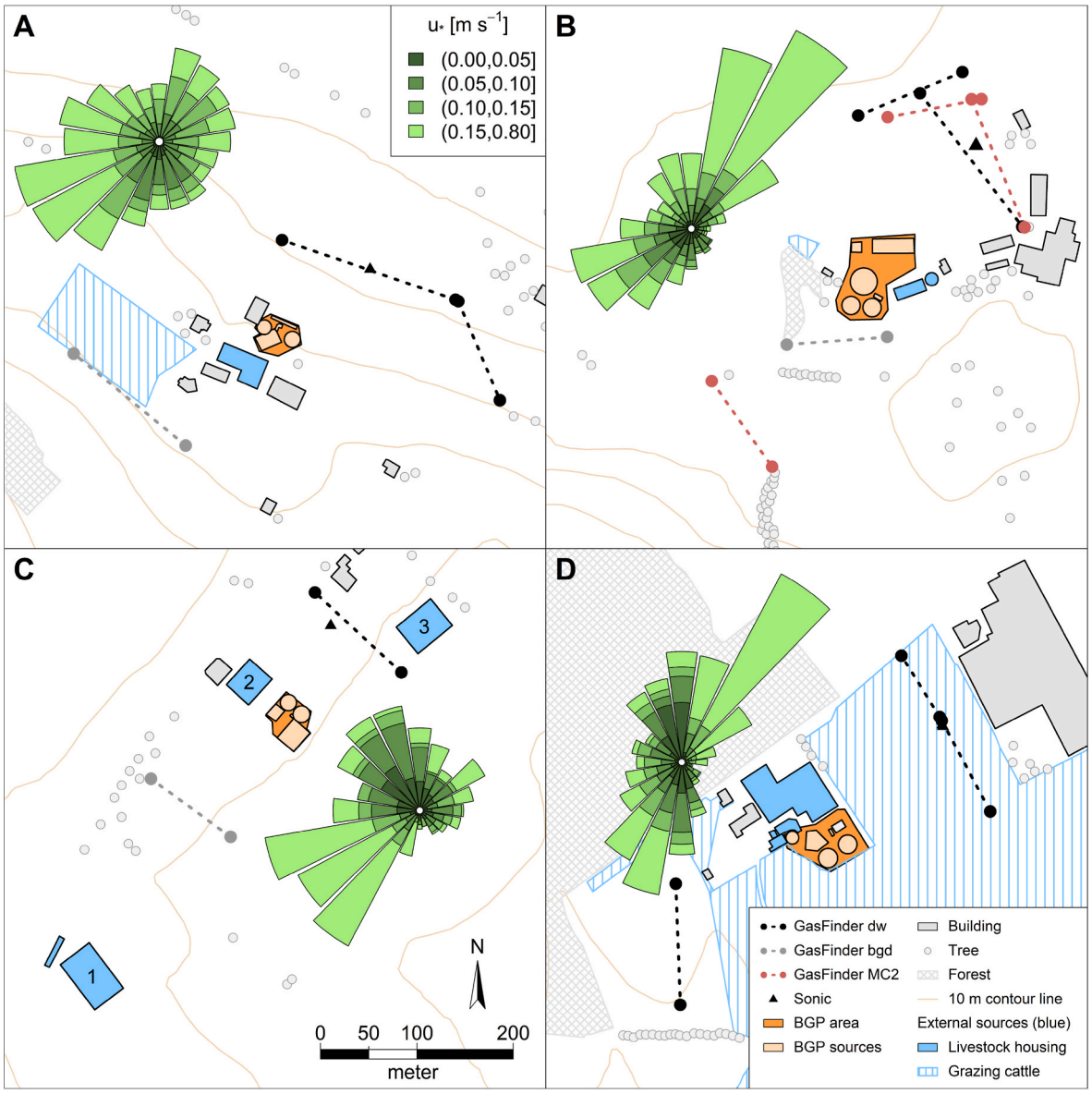

Fig. 2. Schematic overview of BGPs with wind roses. A = BGP-1, B = BGP-2, C = BGP-3, D = BGP-4. The wind rose indicates the frequency of occurrence of wind directions and the friction velocity u_* in each wind direction sector. For BGP-1 and BGP-2, the wind data from both measuring campaigns are plotted. For BGP-2, the positions of the GasFinders for the second campaign (MC2), which differed substantially from those of campaigns one, are plotted in red. For MC2 of BGP-2, emissions were calculated with southwesterly and northeasterly winds. For BGP-4, there was also the intention to measure emissions with southwesterly and northeasterly winds. For BGP-2, the resting place for the cattle within the pasture and for BGP-1 and BGP-4 the entire pasture is used as external source. (For interpretation of the references to colour in this figure legend, the reader is referred to the Web version of this article.)

Table 2
General characteristics of the BGP operating data. Power size according to energy production. Small: < 1000 MhW, medium: 1000–2000 MhW, large: > 2000 MhW. The BGP area corresponds to the filled orange polygon in Fig. 2.

BGP	Power size	Digestate storage	BGP area [m^2]
BGP-1	small	covered	1,525
BGP-2	large	covered gastight	4,924
BGP-3	medium	covered	1,713
BGP-4	large	uncovered	3,211

measurements for only one wind direction except for BGP-2.2, where we projected the measurements with two prevailing wind directions. The pathlengths of the downwind sensors and the minimal distance between the source and the closest downwind sensor are given in Table 3.

2.2.3. *Turbulence measurements and data filtering*

The turbulence characteristics were recorded with sonic anemometers (Gill Windmaster, Gill Instrument Ltd., Lymington, UK) and the data were corrected for a Gill software bug affecting the magnitude of the vertical wind component (Gill Instruments, 2016). As wind vector rotation, a two-axis coordinate rotation was used. The 10 Hz data were averaged to 30 min periods.

The measuring sites were located in landscapes with rather complex topography that does not fulfil the idealised assumptions (horizontal, homogeneous and flat terrain) of the Monin-Obukhov similarity theory (MOST). Therefore, the bLS model output was filtered to avoid unrealistic and error-prone emission results. For each site, an individual quality filtering was applied. Filters were used for friction velocity (u_*), the standard deviation of the along wind scaled by u_* (σ_u/u_*), the standard deviation of the acrosswind divided by u_* (σ_v/u_*), the Kolmogorov constant of the Lagrangian structure function (C_0), the Obu-

Table 3
Pathlengths and minimal distance between any source and the measuring path for all sites. Several figures indicate more than one path (Fig. 1. 2).

Site	Location of downwind sensor	Downwind path length [m]	Minimal distance to source [m]
WWTP-1	Northeast side	65, 49, 52	106
WWTP-2	South side	64, 59	97
BGP-1.1[a]	Northeast side	145, 125	73
BGP-1.2	Northeast side	190, 111	73
BGP-2.1	Northeast side	125, 176	93
BGP-2.2	Northeast and southwest side	99, 143, 109[b]	107, 146[b]
BGP-3	Northeast side	122	93
BGP-4	Northeast side	75, 107	127

[a] The pathlength of the GasFinder in the north was extended towards west and the pathlength of the GasFinder in the east was reduced compared to BGP-1.1. In Fig. 2A the setting of BGP-1.2 is shown.
[b] Sensor on the southwest side of BGP-2.2 measuring downwind concentration with north-easterly winds.

kohv length (L), the roughness length (z_0), the number of touchdowns within the source area, the dispersion factor (D) and a minimal concentration difference (ΔC) between the upwind (background) and the downwind concentration. The applied quality filtering for each site is given in the Supporting information 1, section 2.

2.3. bLS modelling and post-calculations

2.3.1. bLS model calculations

The IDM is a micrometeorological method that combines measurements of the turbulence parameters that are used in a dispersion model with gas concentration measurements up- and downwind of the spatially confined source.

$$Q = \frac{C_{DW} - C_{UW}}{D} \cdot A \quad (1)$$

Q is the emission of the source (standard SI units kg s^{-1}), C_{UW} and C_{DW} the upwind (background) and downwind concentration (kg m^{-3}) and D the dispersion factor (s m^{-1}) depending on the geometrical configuration of source and sensor as well as on the micrometeorological conditions. To gain emissions in kg s^{-1} the calculations have to be multiplied by the area A (units m^{-2}) of the source.

As dispersion model, a backward Lagrangian stochastic model (bLS) described in Flesch et al. (2004) was used to simulate the dispersion factor D (Eq. (1)) for each individual source and each open-path sensor based on the actual turbulence measurements and the source-sensor geometry. The open-path concentration measurements were approximated by a series of point sensors with a 1-m spacing along the path length. For each of these point sensors and each emission interval, 50,000–250,000 backward trajectories were calculated and analysed for touchdowns within the source area. The simulations were done with the R package bLSmodelR (Häni et al., 2018), available at https://github.com/ChHaeni/bLSmodelR.

2.3.2. Combining multiple sensors

Often, there was more than one GasFinder used at the downwind side of the WWTPs and BGPs. If two or more GasFinders were used at one side, these GasFinders were combined post measurement to a single sensor to cover a larger fraction of the emission plume and to be less prone to erroneous measurements as fluctuations within one device are evened out. For each 30 min interval, the weighted average according to the path length of the sensors over the concentration measurements and D values were taken (Eq. (2)),

$$X_{comb} = \frac{\sum_i^N X_i \cdot P_i}{\sum_i^N P_i} \quad (2)$$

with X either concentration C or dispersion factor D for the corresponding device, P = path length, $comb$ = combined sensor. For the number of touchdowns within a source the numbers were summed up. GasFinders that did not measure a valid CH_4 concentration were ignored and thus not combined with the remaining GasFinder(s).

2.3.3. Combining multiple sources

If the source (e.g., WWTP) consists of multiple sources, different levels of detail on how to calculate the total emission are possible. In the present study we used three approaches.

Table 4
Data used for combining multiple sources with the EHD and EWS approaches for the two WWTPs. The number given in the first column indicates the location of the source in Fig. 1. w_i= relative emission ratio in relation to sludge storage tanks used in Eq. (5). Letters indicate external sources. NA = This source does not exist on at the corresponding WWTP. * = not relevant for combining multiple sources.

No	Source	Area [m^2]		w_i EHD		w_i EWS	
		WWTP-1	WWTP-2	WWTP-1	WWTP-2	WWTP-1	WWTP-2
1	Inlet	NA	123	NA	1.8	NA	0.0
2	Sand trap	163	41	0.5	0.6	0.5	0.8
3	Primary clarifier	808	156	2.4	2.2	0.3	0.3
4	Activated sludge tanks	2258	171	6.7	2.5	0.2	0.3
5	Secondary clarifier	1501	NA	4.5	NA	0.1	NA
6	SBR	NA	1017	NA	14.7	NA	0.2
7	Thickener for primary sludge	92	246	0.3	3.5	0.2	0.3
8	Overflow sludge	320	NA	1.0	NA	0.0	NA
9	Digester	236	NA	0.7	NA	0.1	NA
10	Digester + CHP	NA	274	NA	4.0	NA	3.1
11	**Sludge storage tanks**	**336**	**69**	**1.0**	**1.0**	**1.0**	**1.0**
12	Supernatants	226	69	0.7	1.0	0.1	0.5
13	Balloon for biogas storage	120	151	0.4	2.2	0.0	0.2
14	CHP	44	NA	0.1	NA	1.0	NA
A	Open storage for road sweepings	162	NA	*	*	*	*
B	Sheep barn	NA	285	*	*	*	*

(i) ESP: Emissions with a single polygon. For this approach, the WWTP is treated as a single polygon source that covers all individual sources.
(ii) EHD: Emissions with homogeneous emission densities. For this approach, it is assumed that the individual source areas have equal emission densities (i.e., the same emission per area).
(iii) EWS: Emissions with weighted sources. For this approach, the individual source areas have specified relative emissions.

The different approaches are explained with the example of WWTPs. ESP corresponds to the orange outlined polygon in Fig. 1 and to calculate the emissions, Eq. (1) is used. The approaches EHD and EWS are calculated as follow:

Each emission of an individual source Q_i within the WWTP contributes to the total emission Q_{tot} of the WWTP (Eq. (3)):

$$Q_{tot} = \sum_{i=1}^{N} Q_i \tag{3}$$

We assume that the relative emission strengths w_i to a reference source Q_{ref}, which is a source within the WWTP, are known (Eq. (4)):

$$Q_i = Q_{ref} \cdot w_i \tag{4}$$

With the values for w_i and for the areas A_i of the individual sources, the total emission of the WWTP can be calculated using Eq. (5):

$$Q_{tot} = \frac{\Delta C_{tot}}{\sum_{i=1}^{N} \left(\frac{w_i \cdot D_i}{A_i} \right)} \cdot \sum_{i=1}^{N} w_i \tag{5}$$

The full derivation of Q_{tot} is given in the appendix. Note that the approaches EHD and EWS only differ in the determination of w_i. The w_i and A_i to calculate Q_{tot} with the EHD and EWS approaches are given in Table 4.

The ESP approach was used for the BGPs because their components (storage, digester, CHP, etc) are positioned close to each other and the total extension of the plants is relatively small (Fig. 2). This is not the case for the WWTPs, where the total plant area and the distance between the individual sources is larger. Within a WWTP, the individual sources differ in emission density, e.g., the emissions from the sludge storage tanks are expected to be substantially higher per area than those from the secondary settlers. Thus, the use of specified relative emissions is a more appropriate solution. Therefore, the EWS approach was used to calculate emissions from the WWTPs, although the ESP and EHD approach were also applied, and the calculations compared with the results from the EWS approach.

To calculate the w_i for the EWS, literature data were used. Depending on the source, the emissions from the literature data were scaled to the corresponding WWTP with population equivalent (PE) or with the area. The sludge storage tanks were used as reference sources. The literature data used for the specified emissions are given in the Supporting information 1, section 1.

For the WWTPs a simple sensitivity analysis of the EWS approach was done. For this purpose, the w_i of one individual source was multiplied or divided by a factor of 4, while the other w_i retained the original value. The resulting emission was then compared to the original WWTP emission. For the analysis, we used a factor of 4 because the specified emissions from the literature data are on average about four times larger and four times smaller than the minimum and maximum value, respectively.

2.3.4. Treating external sources

At each site, CH_4 sources occurred in close vicinity not belonging to the WWTPs or BGPs. This is a problem if the influence of the external source's CH_4 emissions on the up- and downwind concentration measurements differ. These emissions need to be corrected for in the emission calculation for the WWTPs and BGPs. The external sources were mostly housed livestock or grazing cattle. This issue is illustrated for the example of BGP-3 (Fig. 2C). A few meters northwest of BGP-3, fattening pigs are housed (polygon 2 in Figs. 2C), 300 m southwest (1) and 130 m northeast (3) of the BGP cattle are housed. The emissions from the external sources (1, 2, 3) confound the concentration measurements and thus alter the determined emission of the BGP. The bLS model simulations also included (in addition to the BGP source polygon) calculations for all external sources. For each GasFinder measuring path (upwind and downwind), the dispersion factor $D_{external\_i}$ was available. Instead of calculating the BGP emission directly with the measured concentration difference (Eq. (1)), the partial effect of the external sources ($Q_{external\_i}$) on the measured concentrations was simulated (Eq. (6)).

$$\Delta C_{external\_i} = D_{external\_i} \cdot \frac{Q_{external\_i}}{A_{external\_i}} \tag{6}$$

The emission from the BGP was then calculated as (Eq. (7)):

$$Q_{BGP} = \frac{\left(C_{DW} - \sum_i \Delta C_{DW\_external\_i} \right) - \left(C_{UW} - \sum_i \Delta C_{UW\_external\_i} \right)}{D} \cdot A_{BGP} \tag{7}$$

Frequently, it was not possible to use the IDM to measure the emissions of the external sources as they were too close to the target source or for other reasons. In such cases, the emissions of the external sources had to be assigned based on literature values. Emissions from enteric fermentation of pigs are based on the national inventory values and for cattle on a model which considers age and energy corrected milk yield (FOEN, 2021b). Emissions factors for manure stores are based on Kupper et al. (2020). These assigned emissions may differ from the gas release occurring in reality and thus induce an uncertainty in the emission in the source being investigated. We assumed a general uncertainty of 20% for the external CH_4 emissions and their $\Delta C_{external}$ values.

For grazing cattle, we used two different approaches to define the source polygon in the bLS model. If the cattle had limited time access to the pasture, we used the entire pasture as source polygon (BGP-1.2 and BGP-4). However, if the animals were outside 24 h a day over a period of several days, we used the area on which they usually rested as source polygon only. This is supported by Kilgour (2012), who found that if cattle are on the pasture all day, they spend about one third of their time grazing and most of the remaining time lying (resting and ruminating).

3. Results

3.1. Emissions from wastewater treatment plants

3.1.1. Overview on emissions

There were 398 and 280 valid half-hourly emission values for WWTP-1 and WWTP-2, respectively. This corresponds to an average data loss of 50% and 53% for WWTP-1 and WWTP-2, respectively, due to quality filtering or GasFinder failure. For both WWTPs, the data loss was two to three times larger during the night than during the day (Fig. 3).

As the amount of valid data was not evenly spread over the course of the day and as there might be a diurnal pattern in the emissions, daily averaged emissions were calculated (Fig. 4). The daily averaged CH_4 emissions ± standard deviation (with the EWS approach) were 0.82 ± 0.15 kg h^{-1} and 0.61 ± 0.08 kg h^{-1}, for WWTP-1 and WWTP-2, respectively. The emissions scaled by population equivalent (PE) were 166 ± 31 g PE^{-1} y^{-1} and 381 ± 17 g PE^{-1} y^{-1} for WWTP-1 and WWTP-2, respectively. The CH_4 emission scaled by chemical oxygen demand (COD) for WWTP-1 was 1.9 g m^{-3} of the inflow or 0.7% of COD. For WWTP-2, it was 4.0 g m^{-3} of the inflow or 1.5% of COD.

Both WWTPs showed a similar emission pattern with lower emissions during the night, highest emission in the morning around 8:00 and then decreasing emission until late afternoon (Fig. 4). Measurement data can be found in Supporting information 2.

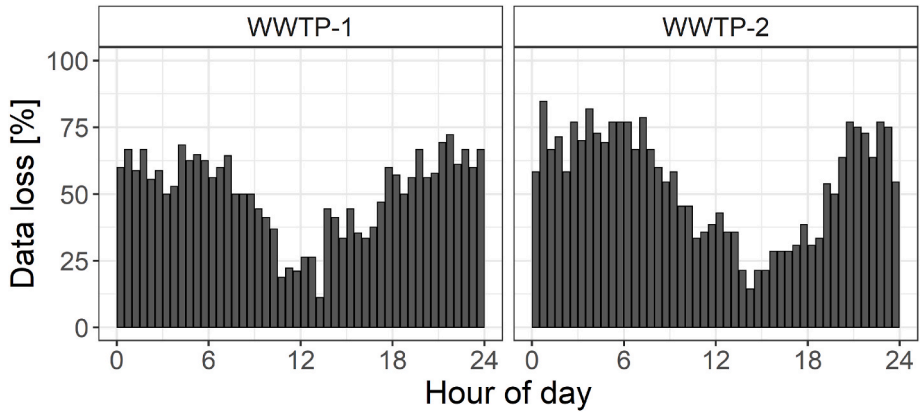

Fig. 3. Proportion of data loss of IDM emission intervals after data filtering given as diurnal cycles for the two WWTPs. Higher bar means higher data loss.

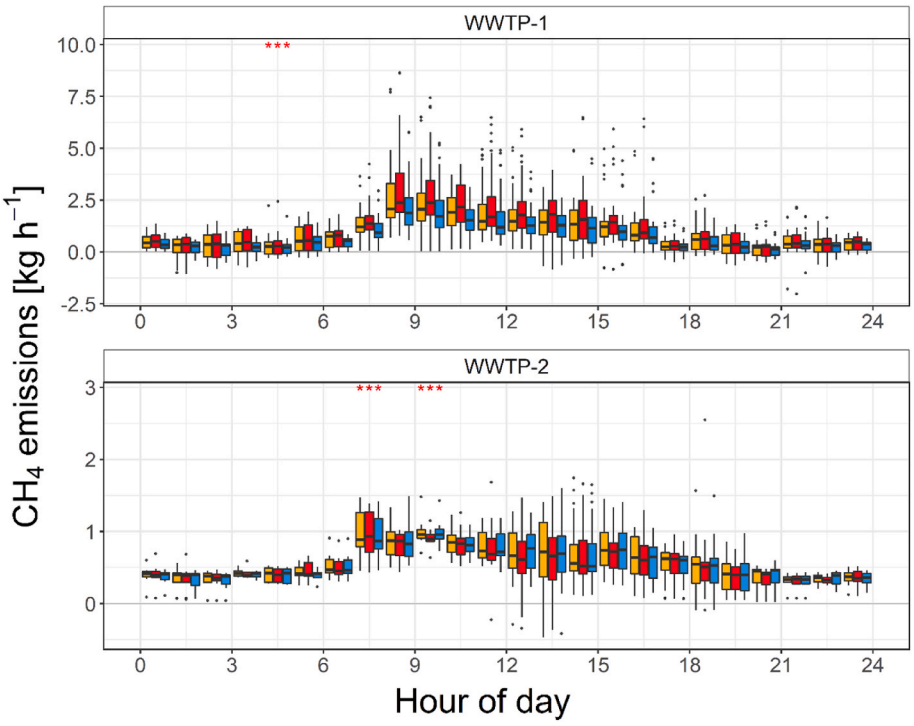

Fig. 4. Diurnal cycle of CH_4 emissions calculated with three different approaches of the two WWTPs plotted as boxplot. ESP (orange), EHD (red) and EWS (blue). The red asterisks indicate outliers that are above 10 kg h^{-1} and 3 kg h^{-1} for WWTP-1 and WWTP-2, respectively. For WWTP-1 there are two outliers per asterisk. ESP (13.58 kg h^{-1} and 14.87 kg h^{-1}), EHD (14.48 kg h^{-1} and 16.24 kg h^{-1}), EWS (12.69 kg h^{-1} and 13.78 kg h^{-1}). For WWTP-2 there is one outlier per asterisk. In chronological order: ESP (6.63 kg h^{-1} and 5.32 kg h^{-1}), EHD (6.54 kg h^{-1} and 5.31 kg h^{-1}), EWS (6.35 kg h^{-1} and 5.04 kg h^{-1}). (For interpretation of the references to colour in this figure legend, the reader is referred to the Web version of this article.)

3.1.2. Combining multiple sources

For both WWTPs, the emissions were calculated with all three approaches in accordance with section 2.3.3. For the ESP approach, the daily averaged emissions for WWTP-1 and WWTP-2 would be 1.01 kg h^{-1} and 0.62 kg h^{-1}, respectively or 202 g PE^{-1} y^{-1} and 388 g PE^{-1} y^{-1}, respectively. For the EHD approach, the daily averaged emissions for WWTP-1 and WWTP-2 would be 1.17 kg h^{-1} and 0.60 kg h^{-1}, respectively or 236 g PE^{-1} y^{-1} and 375 g PE^{-1} y^{-1}, respectively. The diurnal cycles of the two methods are also given in Fig. 4.

The simple sensitivity analysis showed that for WWTP-1, the sources that are most sensitive to the total WWTP emission are the sand trap and the sludge storage tanks. The activated sludge tanks and the primary clarifier have a smaller sensitivity to the total emission. All the other sources have low or no influence on the total emission. For WWTP-2 the source digester + CHP and the sand trap have the biggest sensitivities to the total plant emission. All other sources have only small or negligible influence on the total emission of the WWTP according to the sensitivity analysis (Table 5).

3.2. Emissions from biogas plants

The number of valid half-hourly emission values for the measuring campaigns at BGPs ranged from 78 to 310 and the data loss from 77% to 91%, respectively (Table 6). The average CH_4 emissions varied between 0.44 kg h^{-1} and 2.95 kg h^{-1} and the median CH_4 emissions between 0.39 kg h^{-1} and 2.22 kg h^{-1}. The highest numbers are due to measurements during other than normal operating conditions (OTNOC). The emissions without treatment of external sources are substantially higher for BGP-1, but in a similar range for BGP-2 and lower for BGP-3 than the mean which includes the correction (Table 6). Fig. 5 shows the large variation of hourly emissions of the BGPs.

For BGP-4, the calculation procedure gave predominantly physically implausible results, most likely because of the potentially strong but varying influence of the grazing cattle between the BGP and the concentration measurements. Therefore, no meaningful results can be shown. More information on this issue is provided in section 4.3.1. Measurement data can be found in Supporting information 2.

Table 5
Results of the sensitivity analysis. Percent change in the total WWTP emission if the specified w_i of a single source is increased or decreased by a factor of 4. NA = This source does not exist on the corresponding WWTP.

Source	WWTP-1		WWTP-2	
	Increasing w_i by factor 4	Decreasing w_i by factor 4	Increasing w_i by factor 4	Decreasing w_i by factor 4
Inlet	NA	NA	0%	0%
Sand trap	+17%	−4%	−9%	+4%
Primary clarifier	+11%	−3%	−3%	+1%
Activated sludge tanks	+7%	−2%	−3%	+1%
Secondary clarifier	+2%	0%	NA	NA
SBR	NA	NA	0%	0%
Thickener for primary sludge	0%	0%	0%	0%
Overflow sludge	0%	0%	NA	NA
Digester	−4%	+1%	NA	NA
Digester + CHP	NA	NA	+9%	−6%
Sludge storage tanks	−14%	+26%	0%	0%
Supernatants	+1%	0%	+2%	0%
Balloon for biogas storage	−1%	0%	+2%	0%
CHP	+13%	−3%	NA	NA

3.3. Uncertainty assessment

Bühler et al. (2021) conducted an uncertainty analysis of a measurement campaign with the IDM at an experimental dairy cow housing. They demonstrated that the uncertainty of the average emission decreases with increasing number of observations, i.e., valid emission intervals. As the sites in the present study exhibit similar characteristics regarding topography and micrometeorological conditions as the location used by Bühler et al. (2021) and as the same GasFinders were used, their function to determine the uncertainty was applied for the data of the present study. The resulting random uncertainty ranged from 14% to 21%. However, the sites in the present study exhibit additional (systematic) uncertainties due to external sources and the EWS approach. The total uncertainty for each site was therefore estimated assuming that the uncertainties introduced by the bLS model, external sources and the EWS approach are independent. Using the corresponding values for each site, the total uncertainty in emission of WWTP-1 and WWTP-2 resulted in 36% and 27%, respectively. For the BGPs, the total uncertainties in emissions range from 25% to 30%. Note that in section 3.1.1, the precisions of the daily averaged WWTPs emissions are given and not the uncertainty (or accuracy) calculated here.

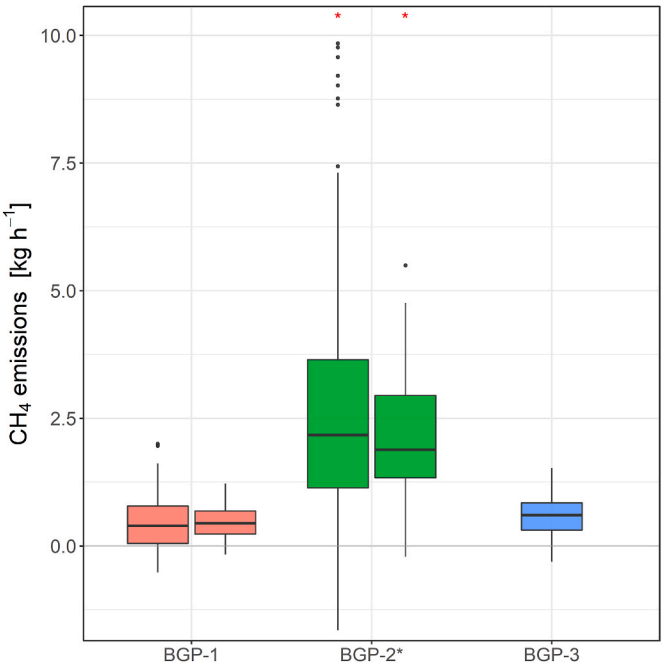

Fig. 5. CH_4 emissions from three different BGPs. For BGP-1 and BGP-2, emissions from two campaigns. The red asterisks indicate outliers that are above 10 kg h^{-1}. There are three outliers for BGP-2.1 (10.77, 11.26, 11.93 kg h^{-1}) and BGP-2.2 (13.48, 21.65, 35.97 kg h^{-1}). BGP-2* measurements were conducted during other than normal operating conditions (OTNOC). (For interpretation of the references to colour in this figure legend, the reader is referred to the Web version of this article.)

4. Discussion

4.1. Wastewater treatment plants

4.1.1. Comparison with literature data

Daelman et al. (2012), Daelman et al. (2013), Delre et al. (2017), Samuelsson et al. (2018), Scheutz and Fredenslund (2019), STOWA (2010) and Yoshida et al. (2014) reported average CH_4 emissions from 16 European WWTPs in the range of 140–1339 g PE^{-1} y^{-1}. The average of these 16 WWTPs was 458 g PE^{-1} y^{-1} (median: 324 g PE^{-1} y^{-1}). Scaled to COD in the influent, the average emissions were 0.9% with a range of 0.3–1.7%. The 16 WWTPs have a size between 40,000 and 805,000 PE and the sewage was mostly of domestic origin. A detailed overview on the emission data of these plants is provided in the Supporting information 1, section 4.

The CH_4 emissions of 177 g PE^{-1} y^{-1} and 420 g PE^{-1} y^{-1} for WWTP-1 and WWTP-2, respectively, lie within the range of the reported literature data. Compared to this data, the emissions of WWTP-1 are at the lower end. In terms of COD in the influent, the emissions of 0.7% and 1.5% compare well with the literature. Overall, the measured emissions observed in the present study are in line with investigations conducted

Table 6
Summary of CH_4 emissions of the BGP-1, BGP-2, and BGP-3 (data not shown for BGP-4; see section 4.3.1).

	BGP-1.1	BGP-1.2	BGP-2.1[a]	BGP-2.2[a]	BGP-3
N of valid values	310	78	143	132	121
Data loss	77%	91%	91%	82%	81%
Median [kg h^{-1}] (with correction for external sources)	0.39	0.44	2.22	1.93	0.60
Mean [kg h^{-1}] (with correction for external sources)	0.44	0.49	2.95	2.61	0.57
SD [kg h^{-1}]	0.50	0.35	2.62	3.69	0.41
Mean [kg h^{-1}] (without correction for external sources)	0.94	0.82	3.23	2.83	0.37

[a] Measurements during other than normal operating conditions (OTNOC) due to a damaged membrane of the fermenter.

previously.

4.1.2. Combining multiple sources

The main problem of the source combination is that the ratios w_i of the specified emissions between the individual sources need to be known. As usually no direct measurement of an individual source is possible with the IDM, these ratios are estimated based on available literature data, which are still sparse and might be uncertain. Additionally, the data need to be scaled to the site. For scaling, we used the PE if possible. This parameter may introduce an additional uncertainty as it depends on the accuracy of the measured WWTP inflow and the COD contents of the sewage. For the digester and the balloon for biogas storage, we made our own assumptions. Despite these challenges, the comparison in section 4.1.1 with the literature showed that the results obtained are reasonable.

For WWTP-2, the differences in total emissions between the ESP and EHD approaches and the EWS approach were 2% and thus of minor importance. But for WWTP-1, the differences were larger. The total CH_4 emission of the ESP approach and the EHD approach were higher by 23% and 43%, respectively, than the EWS approach.

The higher differences between the different approaches in WWTP-1 compared to WWTP-2 are also reflected in the simple sensitivity analysis. For WWTP-1, a change by factor an of four in the w_i of the sludge storage tanks led to a maximum change of 26% in emission, whereas for WWTP-2 the maximum change caused by a single source was 9%. This shows that reliable literature data on the individual sources within a WWTP are important. For the sensitivity analysis, we expected that a change in the emission of the sources with the highest specified emission density would induce the largest change in the total WWTP emission. This was the case for both WWTPs. However, at WWTP-2, the total plant emission is not sensitive to a variation in the specified w_i of the sludge storage tank with the second highest specified emission. The sensitivity analysis of the EWS approach done in the present study suggests that a combination of the location of a source within the source complex, the distance between the emission source and the measurement path, the concentration measurements and the specified emission density (w_i), define the sensitivity. Sources that are rather at the edge of the source complex have a higher sensitivity than sources in its middle. Sources that are closer to the downwind measurement path tend to have a higher sensitivity than those situated further away. But if the w_i of these sources is low, they also have a low sensitivity. The applicability of these findings to other sites needs to be investigated in further studies since additional factors like the position of the GasFinders, the prevailing wind direction, or other micrometeorological parameters may also influence the resulting emission data.

Another reason for the differences between the three approaches for the two WTTPs could be the total WWTP area size. WWTP-1 (21,803 m^2) is about three times larger than WWTP-2 (7,354 m^2) and thus the distance between the different sources is larger. For WWTP-1, the EHD approach had the highest emission and the EWS approach the lowest. This can be explained by the mechanism of the EWS approach: the sludge storage tanks (No 11 on Fig. 1A) are located at the northern corner of the WWTP-1. Southwest of the sludge storage tanks is a larger empty area that is included in the polygon for the ESP approach. For this approach, this configuration allocates more "weight" to the northern part of the WWTP compared to the EHD approach, but less than for the EWS approach. Thus, the emissions with the ESP approach are between the other two approaches.

The question remains as to whether the specified relative emission densities are necessary for the source combination or if a simpler approach could be used. Based on our two examples, we recommend the EWS approach for sources like WWTPs. Additional emission data from individual sources within WWTPs will be available in the future, which might improve the accuracy of the EWS approach.

4.1.3. Interrelations between emission rate and operations at WWTPs

The emissions of individual measurement intervals varied over a large range (Fig. 6). The variability can be due to fluctuations in the gas release from the WWTPs or/and due to varying micrometeorological conditions. Several studies have reported CH_4 emission evolution characterised by a high incidental gas release from slurry storage (i.e. ebullition; (Kaharabata et al., 1998; Baldé et al., 2016). They have shown large variability in gas releases with or without operations at storage tanks. It seems likely that sludge storage tanks, which contribute a large proportion of emissions at the investigated WWTPs, show characteristics regarding emission variability that are similar to those of

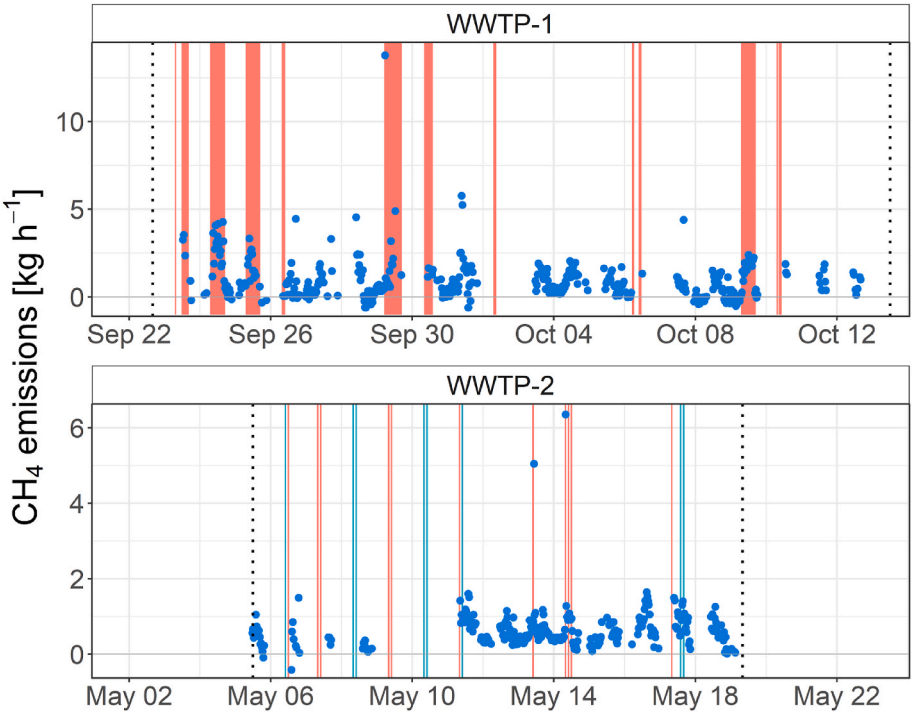

Fig. 6. Interrelations between CH_4 emissions (EWS approach) and agitation of sludge storage tanks and flaring at WWTP-1 and WWTP-2. Red vertical bars indicate the operational time of the agitator of either or both storage tanks. Green vertical bars indicate the flaring periods. The CH_4 emissions are given as 30-min intervals. For WWTP-2, only the starting time of agitation is known and an operation time of 30 min was assumed. Grey dotted vertical lines indicate the start and the end of the measurement campaign. (For interpretation of the references to colour in this figure legend, the reader is referred to the Web version of this article.)

slurry storage tanks on livestock farms. The temporal variability in CH_4 emission observed here is within the range observed in previous studies e.g. conducted at farm sites (Flesch et al., 2005). We investigated interrelations between more than 100 parameters from the operational system and CH_4 emissions at WWTP-1. Having selected those related to activities potentially influencing the gas release of CH_4, we identified several parameters associated with sludge treatment that coincided with emission peaks. Fig. 6 shows a coincidence for periods with the agitation of sludge in either or both storage tanks and CH_4 emission peaks. Other parameters with interrelations are, for example the filling level of the sludge storage tank or the removal of sludge from the tank (not shown). Parameters related to the energy line (e.g. flaring, the volume of biogas storage balloon) did not coincide with CH_4 emission peaks.

For the WWTP-2, numerical data was not available, and we thus employed a visual analysis of images from agitation and flaring obtained from the operational system of the WWTP. Slurry store agitation mostly occurred over a period of less than 1 h duration between 8:00 and 12:00 in the morning. Fig. 6 shows a coincidence for periods with agitation of the sludge storage tank and flaring with emission peaks in some cases. The agitator was operated on average at a capacity of 70% and the gas torch of 10%, which suggests a relatively low effect on gas release.

Information on other potentially non-negligible emission sources such as leakages, e.g. bursts from pressure relief valves (Reinelt et al., 2017; Nisbet et al., 2020), could play a role in the total emissions at both of the investigated plants but could not be specifically obtained in the present study.

The CH_4 emissions at both WWTPs exhibited a diurnal cycle with a maximum at approximately 9:00 and a second, smaller peak mid-afternoon (Fig. 4). As the pattern is not WWTP-specific, we suggest coincidence with operating activities at the WWTPs and not with micrometeorological conditions. The peak in the morning is partly due to sludge storage tank agitation, although this did not occur every day. Another reason for the peak in the morning could be the CH_4 emissions from the sewer system. CH_4 builds up in the sediments and in the biofilm of the sewer system (Mannina et al., 2018) where CH_4 production is higher with longer retention time of the wastewater in the sewer system (Guisasola et al., 2008). During the night, the influent into the WWTPs was small and thus CH_4 could have built up in the sewer system that was then released in the morning leading to an emission peak. There were no operational activities at the WWTPs during the night and therefore the emissions were low.

The observed variability indicates that for a reliable emission estimate, measurement campaigns of sufficient duration are required. Based on our experience, we recommend measuring beyond 10 consecutive days (Bühler et al., 2021) not only to ensure data acquisition under different micrometeorological conditions and the distinct diurnal cycle, but also to compensate for an eventual data loss of more than 60%.

4.1.4. Source apportionment

With the bLS model, it is not possible to distinguish between individual sources within a source complex. Therefore, we evaluated the feasibility of source apportionment based on literature data. Literature data were not available for CH_4 emissions from sludge storage tanks. Due to the similarity of human and pig excretions (both human and pigs are monogastric), data from pig slurry storage (Kupper et al., 2020) corrected for the lower methanisation potential when anaerobically digested (VanderZaag et al., 2018) were used as a proxy for emissions from stored sewage sludge. Based on these data, the estimated proportion of CH_4 emissions originating from sludge storage tanks was 48% and 13% of the total emissions for WWTP-1 and WWTP-2, respectively. The results of WWTP-1 coincide with findings from the literature (STOWA, 2010; Daelman et al., 2012; Delre et al., 2017; Samuelsson et al., 2018) that suggest the sludge line as main CH_4 source. WWTP-2 exhibits a substantially lower value. Given that a much higher emission share for the water line is implausible, we hypothesise that other sources occurred, such as leakage from digestors, gas pipes or the CHP. Liebetrau et al. (2013) found emissions from the CHP ranging from 0.04% to 3.28% (average: 1.74%) of the utilised CH_4 at BGPs. Principally, the same technology is used for the CHP at WWTPs and it can be assumed that CH_4 losses are similar at BGPs and WWTPs. We used the average value 1.74% from Liebetrau et al. (2013) of the gas production and the gas production data from Table 1. This yields CH_4 releases from the CHP of 3,493 kg CH_4 y^{-1} and 1,862 kg CH_4 y^{-1} for WWTP-1 and WWTP-2, respectively. This corresponds to a share relative to the total WWTP emissions of 48% and 35% for WWTP-1 and WWTP-2, respectively. The emissions from the sludge tanks and the CHP combined give 96% and 48% of the total plant emissions for WWTP-1 and WWTP-2, respectively, which is in the range of values for the sludge line found in the literature with WWTP-1 at the higher and WWTP-2 at the lower end. We thus assume that the emissions from the CHP at WWTP-1 are rather in the lower range of the reported values of Liebetrau et al. (2013) for the CHP and vice versa for the WWTP-2. A higher contribution of the CHP leakage for the latter is supported by the lower effect of the sludge storage tank agitation on CH_4 emission and the lower variability of the hourly emissions (Fig. 6). This suggests a continuous CH_4 flow which levels out emission peaks due to operations at the sludge and energy line. With the assumptions above regarding leakage from CHP, both plants would achieve a contribution from the sludge line to the total CH_4 WWTP emissions in the range of 60–80%, which we believe to be plausible.

4.1.5. Calculated emissions below zero

Emissions below zero occur, if after the treatment of potential external sources confounding any concentration measurement, the upwind concentration is higher than the downwind concentration. These negative emissions are solely due to calculations and should not be understood as deposition of CH_4. For WWTP-1, 12% of the emissions were below zero (49 intervals). Most of the intervals (33) were in the time periods September 29, 2019 14:00 – September 29, 2019 23:00 and October 8, 2019 22:00 – October 10, 2019 08:00. The occurrence of an unknown external source emitting and confounding the upwind concentration over these time periods is rather unlikely. We also analysed all filtering parameters and could not find any reason to allow exclusion of these periods.

According to Häni et al. (2021), negative emissions can occur for statistical reasons due to low concentration differences between the up- and downwind measurements. They describe an uncertainty range of the used GasFinders between 2.1 ppm-m and 10.6 ppm-m and report drifts and jumps in the concentration measurements that could be indistinguishable from real concentration fluctuations without an external reference device. Such jumps or drifts could lead to systematic errors.

As we did not have a second GasFinder or another measuring device placed upwind, we were not able to verify whether the upwind sensor was influenced by any external CH_4 source or if a problem with the GasFinder occurred. Nevertheless, we decided to retain these two periods in the data set because removing or excluding such calculated below zero emissions could unintentionally increase the emission of the measured source: without these two periods, the CH_4 emission of WWTP-1 would be higher by 14%.

4.2. Biogas plants

For all BGPs except BGP-2.2, emission measurements were conducted for one wind direction sector only (Table 3). For BGP-2.2, measurements with two prevailing wind directions were possible as we placed the GasFinder at the southwest side further away compared to BGP-2.1 (Fig. 2). The reasons for only one general wind direction at the other BGPs were either the topography, the surrounding sources or lack of wind from more than one direction that would fulfil the filter criteria.

The relative fugitive CH_4 emissions of the BGPs in the present study were lower than 5% of the plants' CH_4 production. This is in line with literature data based on measurements with IDM and GasFinder-2 from

agricultural biogas plants which have reported a range of 1.7–5.2% of fugitive emissions (Flesch et al., 2011; Groth et al., 2015; Hrad et al., 2015). A detailed literature review on BGPs emission (agricultural and non-agricultural) with different measuring techniques including IDM and tracer gas dispersion method is given in Bakkaloglu et al. (2021).

The highest emissions were measured at BGP-2 with some very high emission intervals (Fig. 5). First, this BGP has a large electrical power production and second, according to the operator of the plant, there were other than normal operating conditions during both measuring campaigns due to a damaged membrane of the fermenter. Nevertheless, the relative fugitive emissions still lie within the range of literature data.

In contrast to the WWTPs, we used the ESP approach for the BGPs in the bLS model calculations. This is reasonable as the dimensions of the polygon of the BGPs are 1.5–4.8 times smaller than that of WWTP-2, which showed only small differences of <2% between the different approaches. Further, we believe that due to the open storage of substrate material in the BGPs and due to pipes running between the individual plant parts that could potentially have gas leakage, the assumption of a large polygon is warranted. For larger BGPs with more physical distance between individual parts, it might be preferable to use the EWS approach.

In contrast to the WWTPs, the BGPs did not exhibit a clear diurnal emission pattern and we therefore did not use a diurnal cycle to calculate daily mean emissions. We suggest using the median value to determine emission rates for BGPs to give outliers less weight (Fig. 5). Emissions below zero are caused by small concentration differences between up- and downwind measurements in combination with the uncertainty of the GasFinders and the correction for external sources. However, excluding them would unintentionally increase the emissions as variations might also occur towards high emissions. As for WWTPs, we recommend measurements beyond 10 consecutive days for a reliable emission estimate. This is considerably longer than previous measurement campaigns from whole BGPs that have usually lasted from only hours to a few days (Groth et al., 2015; Reinelt et al., 2017; Clauss et al., 2019; Hrad et al., 2021).

4.3. Coping with complex source configurations

4.3.1. Treatment of external sources

CH_4 sources outside of WWTPs or BGPs occurring at all sites and confounding the concentration measurements could be corrected for. The greater the distance between these sources and the GasFinder paths, the more accurate the results obtained. The biggest problem was emissions from grazing cattle, especially if they were close to the measurement paths. This was one reason for unsuccessful measurements at BGP-4. At this site, there were about 90 grazing dairy cows and 25 heifers on the pastures around the BGP, including the pasture where the GasFinders were placed. The assumption of homogeneous emissions from such a large area differed strongly from reality and thus produced obviously erroneous results with the bLS model calculations. The effect of external sources very much depended on their position relative to the wind direction and to the measurement locations. For WWTP-1 and WWTP-2, emissions without correction for external source would be higher by 27% and lower by 4%, respectively. The average emissions of BGP-1.1 and BGP-1.2 without correction of external sources would be higher by 114% and 67%, respectively, and for BGP-2.1 and BGP-2.2, by 10% and 8%, respectively. For BGP-3, the emissions without treatment of external sources would be lower by 35%. For WWTP-1, BGP-1 and BGP-2, the external sources predominantly influenced the downwind concentration and thus, the emissions without treatment of external sources would be higher. At WWTP-2, the sheep barn at the northern side mostly influenced the upwind concentration and only to a smaller extent the downwind concentration. At BGP-3, the emission from the fattening pigs' housing exclusively influenced the downwind concentration, however the dairy cow housing northeast of the BGP (Fig. 2C) produced higher CH_4 emissions and as a consequence, the CH_4 upwind concentration was more confounded than the downwind concentration. Thus, for these two sites the emissions without treatment of external sources would be lower.

Correcting for external sources introduces an additional uncertainty for the WWTP and BGP emissions. For the external sources, we assume a general uncertainty of the $\Delta C_{external\_i}$ (Eq. (6)) of 20%. The larger the share of $\Delta C_{external}$ in the $\Delta C_{measured}$, the larger the uncertainty of the plant emissions. A change in 20% in emissions of the external sources would result in a change in WWTP-1 and WWTP-2 emission of 6% and 1%, respectively. For BGP-1.1, BGP-1.2, BGP-2.1, BGP-2.2 and BGP-3, the changes in the average emission would be 19%, 14%, 2%, 2% and 7%, respectively.

The higher numbers for BGP-1 are due to the small distance between the external sources and the BGP and the similar amount of CH_4 production of both. These considerations regarding uncertainty suggest that the treatment of external sources allows an accurate correction thereof as the resulting data are comparable with emissions obtained from other studies.

4.3.2. Placement of concentration sensors

At WWTP-1, measurements were only possible with south-westerly winds due to the mound southwest of the WWTP. The background sensor was placed close to the mound as there were grazing heifers between the mound and the WWTP. At WTTP-2 we knew from previous turbulence measurements that data passing filtering would be unlikely with wind from south (e.g., too low wind speeds) and thus we planned only measurements with northerly winds. At BGP-1, measurements with northeast wind were not possible due to the forest and the pasture. There was mostly northeast wind during the first campaign at BGP-2 and so we placed the GasFinder for the second campaign at the southwest side further away from the plant to enable measuring from the two prevailing wind directions. Also, the setup of the northeast side was optimised for the local wind directions. At BGP-3, measurements were planned with southwest wind only because cattle housing No 3 (Fig. 2C) would have been too close to the measurement path.

Determining emissions from WWTPs and BGPs at sites with a mostly complex environment as prevails in Switzerland is challenging. Placing GasFinder devices is often hampered due to several different factors that need to be considered. It depends on the borders of the occurring plots, canopy height of the occurring plots, traffic routes, topography (often non-flat), surrounding CH_4 sources and other obstacles like trees or buildings. An analysis of trade-offs between the different factors is necessary, which often results in only one feasible wind direction for measurements: only in two out of seven campaigns was it possible to use data from two general wind directions. A prior determination of the prevailing wind direction is the most important factor. Before each campaign started, we used data from nearby weather stations to determine the wind direction. However, due to non-flat topography and forests, the available data were not always representative for the plant sites. In case of BGP-4, the latter factor was another reason for the unsuccessful results. At this site, the wind direction was not parallel to the forest as previously expected. The wind direction was more towards 180° and therefore caused a wind edge rendering the turbulence measurements not representative for the entire area. Thus, the best case would be to make extended wind measurements directly at the experimental site prior to the campaign.

Another problem could be low concentration differences between the up- and downwind measurements. GasFinders-3 have a relatively large uncertainty (Häni et al., 2021) and therefore sufficient concentration differences are needed. With increasing wind speed and unstable conditions, concentration differences may decrease. This raises the uncertainty of the results and could also lead to calculated emissions below zero. At WWTP-2, we had already conducted a measuring campaign one year prior to the shown measurements that was not successful. We placed the GasFinder on the downwind side too far away from the WWTP with too long measuring paths and thus no concentration

difference between the up- and downwind concentrations was detected. For this reason, the distance between the measuring path and the WWTP-1 shown in Table 3 is rather short.

5. Conclusions

In the present study, CH_4 emission measurements by the IDM of whole WWTPs and BGPs produced reasonable results that are in line with literature data. We demonstrated that reliable emission determination under rather complex conditions is possible. The present study thus provides several valuable insights on how to conduct successful CH_4 measurements with IDM under such challenging situations. It shows that prior analysis of the external sources in combination with the wind direction is important to detect sites where measurements are likely to fail (like BGP-4 with insufficient localisation of grazing cattle, wind edge). After selecting a site, a careful analysis of trade-offs regarding placing measurement devices must be done. Often, a compromise is required between extending the distance toward the source to have the turbulence re-established and limiting it to obtain sufficient difference between the upwind and downwind concentrations. For the measuring campaign itself, sufficient time should be planned, especially where only one general wind direction for measurements is possible. In the present study, we demonstrated a procedure for the treatment of external sources. Furthermore, we introduced an approach for more accurate emission calculations for sources of greater complexity. For this approach, we specified the individual sources within a source complex and calculated the total emission according to these relative weights. We showed that such an approach is necessary for large sources like WWTPs. This approach can be refined with additional available measurement data from individual sources. The future use of source apportionment will provide further experience and thus increase the accuracy of measurements with IDM under complex situations; this also applies for treatment of external sources.

CRediT authorship contribution statement

Marcel Bühler: Software, Investigation, Writing – original draft, Writing – review & editing, Visualization. **Christoph Häni:** Methodology, Software. **Christof Ammann:** Writing – review & editing, Supervision. **Stefan Brönnimann:** Supervision. **Thomas Kupper:** Conceptualization, Writing – review & editing, Supervision, Project administration, Funding acquisition.

Declaration of competing interest

The authors declare that they have no known competing financial interests or personal relationships that could have appeared to influence the work reported in this paper.

Acknowledgements

Funding from the Swiss Federal Office for the Environment (contract number: 06.0091.PZ/R281-0748) for the project regarding wastewater treatment plants is gratefully acknowledged. This work was also supported by the Swiss Federal Office of Energy (contract number: SI/501679-01) and the Swiss Federal Office for the Environment (contract number: 17.0083.PJ/R035-0703) as part of the 'Evaluation and reduction of methane emissions from different European biogas plant concepts' (EvEmBi) project. We are grateful to Ökostrom Schweiz for the valuable input and discussions regarding biogas plants. We thank the operators of the wastewater treatment plants, biogas plants and the farmers of the land in the surrounding areas. We thank Martin Häberli-Wyss (School of Agricultural, Forest and Food Sciences, Zollikofen) for his support and assistance during the measurements and Albrecht Neftel (Neftel Research Expertise, Wohlen bei Bern) for his highly valuable support. We thank Elizabeth Steele (School of Agricultural, Forest and Food Sciences, Zollikofen) for proofreading.

Appendix A. Supplementary data

Supplementary data to this article can be found online at https://doi.org/10.1016/j.aeaoa.2022.100161.

A. Appendix.

Here we give the derivation on how to combine multiple sources.

A. Combining multiple sources

We have calculated D_i (h m^{-1}) values that are a function of the micrometeorological parameters and the source-sensor geometry for N sources. We intend to combine all N sources into one source with an average emission of Q_{tot}. The emission of a sources Q_i (with unit kg h^{-1}) is defined as:

$$Q_i = E_i \cdot A_i \tag{A1}$$

where E is the emission density (kg m^{-2} h^{-1}) and A (m^2) the area of the source.

Each source Q_i contributes to the total emission Q_{tot}

$$Q_{tot} = \sum_{i=1}^{N} Q_i \tag{A2}$$

Assumption: The relative emission strengths w_i to a reference source Q_{ref}, which is a source within the source complex, are known:

$$Q_i = Q_{ref} \cdot w_i \tag{A3}$$

Expanding Eq. (A3) gives

$$Q_i = E_{ref} \cdot A_{ref} \cdot w_i \tag{A4}$$

Combining Eq. (A1)-A4 results in

$$Q_{tot} = E_{ref} \cdot A_{ref} \cdot \sum_{i=1}^{N} w_i \tag{A5}$$

The bLS model simulates the dispersion factor D_i between each individual source E_i and its partial concentration effect ΔC_i:

$$\Delta C_i = D_i \cdot E_i \tag{A6}$$

The measured concentration difference is a sum (superposition) of the individual concentration effects of all sources:

$$\Delta C_{tot} = \sum_{i=1}^{N} \Delta C_i \tag{A7}$$

Combining Eq. (A3), A4, A6 and A7

$$\Delta C_{tot} = E_{ref} \cdot A_{ref} \cdot \sum_{i=1}^{N} \left(\frac{w_i \cdot D_i}{A_i} \right) \tag{A8}$$

Solving for E_{ref}

$$E_{ref} = \frac{\Delta C_{tot}}{A_{ref} \cdot \sum_{i=1}^{N} \left(\frac{w_i \cdot D_i}{A_i} \right)} \tag{A9}$$

Once E_{ref} is known, the emission of the total source complex can be calculated.

$$Q_{tot} = \frac{\Delta C_{tot}}{\sum_{i=1}^{N} \left(\frac{w_i \cdot D_i}{A_i} \right)} \cdot \sum_{i=1}^{N} w_i \tag{A10}$$

Note that as the weights w_i are defined in relation to Q_i, they are different for the EHD and EWS approaches. In Table 4, the w_i for the two approaches are given.

In the EHD approach, the w_i are reduced to the ratio of the areas, so Eq. (A10) can be reduced to:

$$Q_{tot} = \frac{\Delta C_{tot}}{\sum_{i=1}^{N} D_i} \cdot \sum_{i=1}^{N} A_i \tag{A11}$$

References

Bakkaloglu, S., Lowry, D., Fisher, R.E., France, J.L., Brunner, D., Chen, H., Nisbet, E.G., 2021. Quantification of methane emissions from UK biogas plants. Waste Manag. 124, 82–93.

Baldé, H., VanderZaag, A.C., Burtt, S., Evans, L., Wagner-Riddle, C., Desjardins, R.L., MacDonald, J.D., 2016. Measured versus modeled methane emissions from separated liquid dairy manure show large model underestimates. Agric. Ecosyst. Environ. 230, 261–270.

Bühler, M., Häni, C., Ammann, C., Mohn, J., Neftel, A., Schrade, S., Zähner, M., Zeyer, K., Brönnimann, S., Kupper, T., 2021. Assessment of the inverse dispersion method for the determination of methane emissions from a dairy housing. Agric. For. Meteorol. 307, 108501.

Clauss, T., Reinelt, T., Liebetrau, J., Vesenmaier, A., Reiser, M., Flandorfer, C., Stenzel, S., Piringer, M., Fredenslund, A.M., Scheutz, C., Hrad, M., Ottner, R., Huber-Humer, M., Innocenti, F., Holmgren, M., Yngvesson, J., 2019. Recommendations for Reliable Methane Emission Rate Quantification at Biogas Plants, vol. 33. DBFZ-Report, Leipzig.

Daelman, M.R.J., van Voorthuizen, E.M., van Dongen, L.G.J.M., Volcke, E.I.P., van Loosdrecht, M.C.M., 2013. Methane and nitrous oxide emissions from municipal wastewater treatment - results from a long-term study. Water Sci. Technol. 67, 2350–2355.

Daelman, M.R.J., van Voorthuizen, E.M., van Dongen, U.G.J.M., Volcke, E.I.P., van Loosdrecht, M.C.M., 2012. Methane emission during municipal wastewater treatment. Water Res. 46, 3657–3670.

Delre, A., Mønster, J., Scheutz, C., 2017. Greenhouse gas emission quantification from wastewater treatment plants, using a tracer gas dispersion method. Sci. Total Environ. 605–606, 258–268.

Eijo-Río, E., Petit-Boix, A., Villalba, G., Suárez-Ojeda, M.E., Marin, D., Amores, M.J., Aldea, X., Rieradevall, J., Gabarrell, X., 2015. Municipal sewer networks as sources of nitrous oxide, methane and hydrogen sulphide emissions: a review and case studies. J. Environ. Chem. Eng. 3, 2084–2094.

Flesch, T.K., Desjardins, R.L., Worth, D., 2011. Fugitive methane emissions from an agricultural biodigester. Biomass Bioenergy 35, 3927–3935.

Flesch, T.K., Vergé, X.P.C., Desjardins, R.L., Worth, D., 2013. Methane emissions from a swine manure tank in western Canada. Can. J. Anim. Sci. 93, 159–169.

Flesch, T.K., Wilson, J.D., Harper, L.A., Crenna, B.P., 2005. Estimating gas emissions from a farm with an inverse-dispersion technique. Atmos. Environ. 39, 4863–4874.

Flesch, T.K., Wilson, J.D., Harper, L.A., Crenna, B.P., Sharpe, R.R., 2004. Deducing ground-to-air emissions from observed trace gas concentrations: a field trial. J. Appl. Meteorol. 43, 487–502.

FOEN, 2021a. Emission von Treibhausgasen nach CO_2-Gesetz und Kyoto-Protokoll, 2. Verpflichtungsperiode (2013-2020). Federal Office for the Environment FOEN, Bern. https://www.bafu.admin.ch/dam/bafu/de/dokumente/klima/fachinfo-daten/CO2_Statistik.pdf.download.pdf/CO2_Publikation_de_2021-07.pdf. (Accessed 3 August 2021).

FOEN, 2021b. Switzerland's Greenhouse Gas Inventory 1990-2019, National Inventory Report: Including Reporting Elements under the Kyoto Protocol. Submission of April 2021 under the United Nations Framework Convention on Climate Change and under the Kyoto Protocol. Federal Office for the Environment FOEN, Bern. https://www.bafu.admin.ch/dam/bafu/en/dokumente/klima/klima-climatereporting/National_Inventory_Report_CHE.pdf.download.pdf/National_Inventory_Report_CHE_2021.pdf. (Accessed 5 August 2021).

Gill Instruments, 2016. Technical Key Note: Software Bug Affecting 'w' Wind Component of the WindMaster Family. Gill Instruments, Lymington, UK. http://gillinstruments.com/data/manuals/KN1509_WindMaster_WBug_info.pdf.

Groth, A., Maurer, C., Reiser, M., Kranert, M., 2015. Determination of methane emission rates on a biogas plant using data from laser absorption spectrometry. Bioresour. Technol. 178, 359–361.

Guisasola, A., Haas, D. de, Keller, J., Yuan, Z., 2008. Methane formation in sewer systems. Water Res. 42, 1421–1430.

Gujer, W., 2007. Siedlungswasserwirtschaft, third ed., vol. XV. Springer-Verlag Berlin Heidelberg, p. 431 S.

Häni, C., Bühler, M., Neftel, A., Ammann, C., Kupper, T., 2021. Performance of open-path GasFinder3 devices for CH_4 concentration measurements close to ambient levels. Atmos. Meas. Tech. 14, 1733–1741.

Häni, C., Flechard, C., Neftel, A., Sintermann, J., Kupper, T., 2018. Accounting for field-scale dry deposition in backward Lagrangian stochastic dispersion modelling of NH_3 emissions. Atmosphere 9, 146.

Harper, L.A., Denmead, O.T., Flesch, T.K., 2011. Micrometeorological techniques for measurement of enteric greenhouse gas emissions. Anim. Feed Sci. Technol. 166–167, 227–239.

Hrad, M., Piringer, M., Huber-Humer, M., 2015. Determining methane emissions from biogas plants–Operational and meteorological aspects. Bioresour. Technol. 191, 234–243.

Hrad, M., Vesenmaier, A., Flandorfer, C., Piringer, M., Stenzel, S., Huber-Humer, M., 2021. Comparison of forward and backward Lagrangian transport modelling to determine methane emissions from anaerobic digestion facilities. Atmos. Environ. X 12, 100131.

Kaharabata, S.K., Schuepp, P.H., Desjardins, R.L., 1998. Methane emissions from above ground open manure slurry tanks. Global Biogeochem. Cycles 12, 545–554.

Kilgour, R.J., 2012. In pursuit of "normal": a review of the behaviour of cattle at pasture. Appl. Anim. Behav. Sci. 138, 1–11.

Kupper, T., Häni, C., Neftel, A., Kincaid, C., Bühler, M., Amon, B., VanderZaag, A., 2020. Ammonia and greenhouse gas emissions from slurry storage - a review. Agric. Ecosyst. Environ. 300, 106963.

Liebetrau, J., Reinelt, T., Clemens, J., Hafermann, C., Friehe, J., Weiland, P., 2013. Analysis of greenhouse gas emissions from 10 biogas plants within the agricultural sector. Water Sci. Technol. 67, 1370–1379.

Mannina, G., Butler, D., Benedetti, L., Deletic, A., Fowdar, H., Fu, G., Kleidorfer, M., McCarthy, D., Steen Mikkelsen, P., Rauch, W., Sweetapple, C., Vezzaro, L., Yuan, Z., Willems, P., 2018. Greenhouse gas emissions from integrated urban drainage systems: where do we stand? J. Hydrol. 559, 307–314.

Nisbet, E.G., Fisher, R.E., Lowry, D., France, J.L., Allen, G., Bakkaloglu, S., Broderick, T. J., Cain, M., Coleman, M., Fernandez, J., Forster, G., Griffiths, P.T., Iverach, C.P., Kelly, B.F.J., Manning, M.R., Nisbet-Jones, P.B.R., Pyle, J.A., Townsend-Small, A., al-Shalaan, A., Warwick, N., Zazzeri, G., 2020. Methane mitigation: methods to reduce emissions, on the path to the paris agreement. Rev. Geophys. 58.

Reinelt, T., Delre, A., Westerkamp, T., Holmgren, M.A., Liebetrau, J., Scheutz, C., 2017. Comparative use of different emission measurement approaches to determine methane emissions from a biogas plant. Waste Manag. 68, 173–185.

Samuelsson, J., Delre, A., Tumlin, S., Hadi, S., Offerle, B., Scheutz, C., 2018. Optical technologies applied alongside on-site and remote approaches for climate gas emission quantification at a wastewater treatment plant. Water Res. 131, 299–309.

Scheutz, C., Fredenslund, A.M., 2019. Total methane emission rates and losses from 23 biogas plants. Waste Manag. 97, 38–46.

Stocker, T.F., Qin, D., Plattner, G.-K., Alexander, L.V., Allen, S.K., Bindoff, N., Bréon, F.-M., Church, J.A., Cubasch, U., Emori, S., Forster, P., Friedlingstein, P., Gillett, N., Gregory, J.M., Hartmann, D.L., Jansen, E., Kirtman, B., Knutti, R., Krishna Kumar, K., Lemke, P., Marotzke, J., Masson-Delmotte, V., Meehl, G.A., Mokhov, I.I., Piao, S., Ramaswamy, V., Randall, D., Rhein, M., Rojas, M., Sabine, C., Shindell, D., Talley, L.D., Vaughan, D.G., Xie, S.-P., 2013. Technical summary. In: Climate Change 2013: the Physical Science Basis. Contribution of Working Group I to the Fifth Assessment Report of the Intergovernmental Panel on Climate Change, Cambridge, United Kingdom and New York, NY, USA.

STOWA, 2010. Emissies Van Broeikasgassen Van RWZI's, Amersfoort, the Netherlands.

VanderZaag, A.C., Baldé, H., Crolla, A., Gordon, R.J., Ngwabie, N.M., Wagner-Riddle, C., Desjardins, R., MacDonald, J.D., 2018. Potential methane emission reductions for two manure treatment technologies. Environ. Technol. 39, 851–858.

VanderZaag, A.C., Flesch, T.K., Desjardins, R.L., Baldé, H., Wright, T., 2014. Measuring methane emissions from two dairy farms: seasonal and manure-management effects. Agric. For. Meteorol. 194, 259–267.

Yoshida, H., Mønster, J., Scheutz, C., 2014. Plant-integrated measurement of greenhouse gas emissions from a municipal wastewater treatment plant. Water Res. 61, 108–118.